Convective Mass Transfer in the Presence of Polarizing Fields: Dispersion in Hollow Fiber Electropolarization Chromatography

JOAQUIM F. G. REIS
DORAISWAMY RAMKRISHNA
and
EDWIN N. LIGHTFOOT
Department of Chemical Engineering
University of Wisconsin
Madison, Wisconsin 53706

An effective means is developed for describing two-dimensional convective dispersion in the presence of polarizing fields. Explicit results are given for planar fields applied across Poiseuille flows, and these are used to characterize hollow fiber electropolarization chromatography (EPC).

SCOPE

Functional analysis is used to extend Taylor dispersion theory to two-dimensional problems in which solute dispersion is biased by polarizing fields or flows. Explicit results are given for combinations of planar fields and Poiseuille flows using an extension of the technique of Gill and Sankarasubramanian. These are sufficiently detailed for preliminary design of hollow fiber chromatography and a variety of related physical operations.

CONCLUSIONS AND SIGNIFICANCE

The numerical results of this study establish the attractiveness of EPC as a separations tool and provide a basis for preliminary design calculations. They also show that much simpler boundary-layer approximations will be adequate for many calculations and establish the useful range of these approximations.

These results also describe other situations of possible physical interest, including both other forms of polarization chromatography and the gravitational settling of suspensions in duct flow.

The mathematical technique used represents a significant extension of Taylor dispersion theory, and it can be extended to more complex fields and flows than considered here. From a purely mathematical standpoint, it is a useful example of the application of functional analysis for extension of Sturm-Liouville theory to two-dimensional problems.

Electropolarization chromatography in a cylindrical duct, or hollow fiber EPC has been described elsewhere (Reis and Lightfoot, 1976). This system consists essentially of an anisotropic ultrafiltration hollow fiber of circular cross section bathed in a circulating buffer solution and subjected to a transverse electrical field. In operation, carrier electrolyte flows through the fiber lumen, that is, in the z direction (see Figure 1), continuously, and a pulse of the polyelectrolyte mixture to be separated is introduced at the feed end ($z = 0$) to initiate the separation.

The electric field, applied in the y direction, induces the polarization of the charged proteins, that is, a nonuniform distribution over the column cross section, as indicated in the figure. The axial velocity of a protein pulse may then be represented as

$$\langle v_i \rangle = \frac{\int_S c_i v ds}{\int_S c_i ds} \tag{1}$$

The velocity $\langle v_i \rangle$ is then the velocity of the center of mass of species i.

It will be seen below that the retardation coefficient

$$r_i \equiv \langle v \rangle / \langle v_i \rangle \tag{2}$$

is always greater than unity for a finite field and that r_i increases with the degree of polarization. Separation of any two species is possible when their retardation coefficients differ.

The retardation coefficient and the axial dispersion are the process characteristics of greatest interest in determining the feasibility of separation, and this paper is devoted to their prediction.

The general description of the concentration distribution of species i in the system schematically represented in Figure 1 is

$$\frac{\partial c_i}{\partial t} + v_0\left[1 - \frac{x^2 + y^2}{R^2}\right]\frac{\partial c_i}{\partial z} + m_i\left[E_x\frac{\partial c_i}{\partial x} + E_y\frac{\partial c_i}{\partial y}\right] = \mathcal{D}_{im}\left[\frac{\partial^2 c_i}{\partial x^2} + \frac{\partial^2 c_i}{\partial y^2} + \frac{\partial^2 c_i}{\partial z^2}\right] \tag{3}$$

The first boundary condition which goes with Equation (3) is the statement of zero net flux normal to the wall for each polyelectrolyte; that is

Joaquim F. G. Reis is with the Departmento de Engenharia Quimica, Faculdade de Engenharia, Porto-Portugal. Doraiswamy Ramkrishna is at the School of Engineering, Purdue University, West Lafayette, Indiana 47907.

0001-1541-78-1236-0679-$01.05.

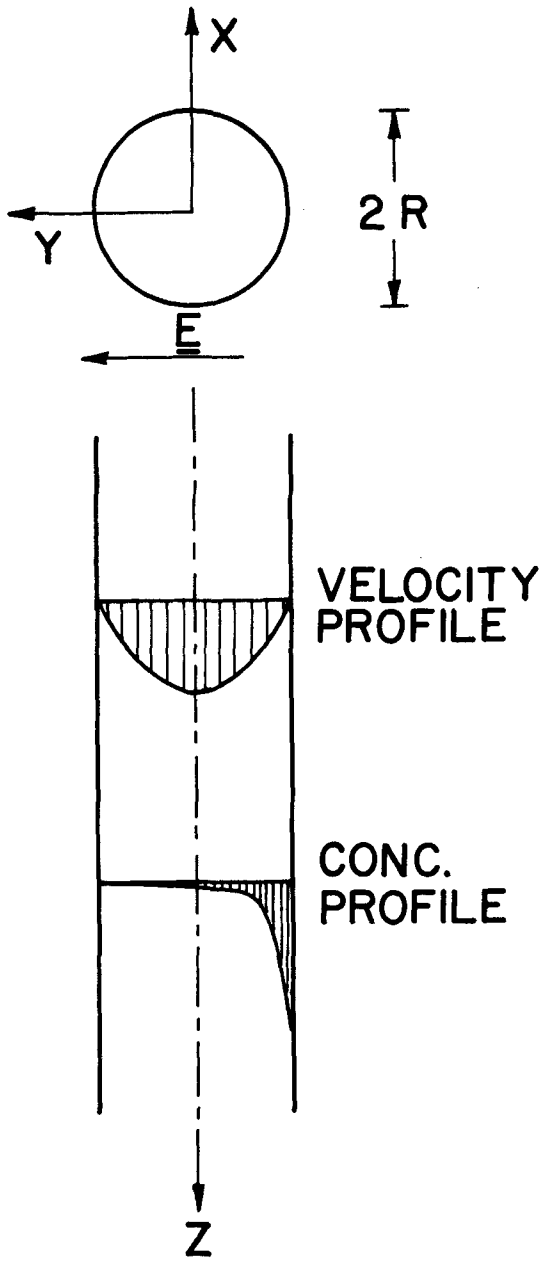

Fig. 1. Hollow fiber EPC: coordinate system, solvent velocity profile, and fully developed concentration profile.

$$m_i\left(\frac{x}{R}E_y+\frac{y}{R}E_x\right)c_i=\mathcal{D}_{im}\left(\frac{x}{R}\frac{\partial c_i}{\partial x}+\frac{y}{R}\frac{\partial c_i}{\partial y}\right)$$
$$\text{at}\quad x^2+y^2=R^2 \qquad (4)$$

The second boundary condition is that the concentration distribution is symmetric with respect to the z-y plane.

As for initial condition, we state that the concentration distribution starts as a pulse in the z direction:

$$c_i=C_i\delta(z) \qquad (5)$$

The spatial distribution of the electrical field inside the hollow fiber is unknown, but it seems reasonable to assume that it is uniform (see Reis and Lightfoot, 1976).

A MODEL FOR HOLLOW FIBER EPC

If the electrical field is uniform and aligned in the y direction, Equations (3) and (4) reduce to

$$\frac{\partial c_i}{\partial t}+v_0\left[1-\frac{x^2+y^2}{R^2}\right]\frac{\partial c_i}{\partial z}+m_iE_y\frac{\partial c_i}{\partial y}=\mathcal{D}_{im}\left[\frac{\partial^2 c_i}{\partial x^2}+\frac{\partial^2 c_i}{\partial y^2}+\frac{\partial^2 c_i}{\partial z^2}\right] \qquad (6)$$

and

$$m_i\left[\frac{x}{R}E_y\right]c_i=\mathcal{D}_{im}\left[\frac{x}{R}\frac{\partial c_i}{\partial x}+\frac{y}{R}\frac{\partial c_i}{\partial y}\right]$$
$$\text{at}\quad x^2+y^2=R^2 \qquad (7)$$

or, introducing a set of dimensionless variables, we get

$$\frac{\partial c_i}{\partial \tau}+(1-\alpha_i-\chi^2-\eta^2)\frac{\partial c_i}{\partial \zeta}+\epsilon_i\frac{\partial c_i}{\partial \eta}=\frac{\partial^2 c_i}{\partial \chi^2}+\frac{\partial^2 c_i}{\partial \eta^2}+\frac{1}{Pe_i^2}\cdot\frac{\partial^2 c_i}{\partial \zeta^2} \qquad (8)$$

and

$$\eta\left(\frac{\partial c_i}{\partial \eta}-\epsilon_i c_i\right)+\chi\frac{\partial c_i}{\partial \chi}=0 \quad \text{at} \quad \chi^2+\eta^2=1 \qquad (9)$$

where α_i is the dimensionless velocity of the center of mass of species i

$$\alpha_i=\frac{\langle v_i\rangle}{v_0}=\frac{1}{v_0}\frac{\int_{-R}^{+R}\int_{-\sqrt{R^2-x^2}}^{+\sqrt{R^2-x^2}}\int_{-\infty}^{+\infty}c_i v\,dz\,dy\,dx}{\int_{-R}^{+R}\int_{-\sqrt{R^2-x^2}}^{+\sqrt{R^2-x^2}}\int_{-\infty}^{+\infty}c_i\,dz\,dy\,dx} \qquad (10, 11)$$

and ζ is the dimensionless axial position relative to the center of mass of species i

$$\zeta=\frac{z/R}{Pe_i}-\int_0^\tau \alpha_i\,d\tau' \qquad (12)$$

FORMAL SOLUTION OF THE CONTINUITY EQUATION, GILL AND SANKARASUBRAMANIAN'S TECHNIQUE

The solution of Equation (8) is based on the following expansion of c_i

$$c_i=\bar{c}_i f_0+\sum_{n=1}^{\infty}\frac{\partial^n \bar{c}_i}{\partial \zeta^n}f_n \qquad (13)$$

where

$$\bar{c}_i\equiv\langle c_i\rangle\equiv\frac{1}{\pi}\int_{-1}^{1}\int_{-\sqrt{1-\eta^2}}^{\sqrt{1-\eta^2}}c_i\,d\chi\,d\eta \qquad (14)$$

used by Gill and Sankarasubramanian (1970) in the solution of dispersion problems. The series (13) is, of course, assumed to converge without proof. In this sense, no justification of Equation (13) is available other than by direct computation. Also, expansion (13) presumes that the concentration variable can be differentiated infinitely many times with respect to ζ everywhere, a stipulation highly in excess of that implied by Equation (8), which demands no more than twice differentiability. We must then infer that, provided the initial condition is cooperative, Equation (13) implies that the concentration profile is analytic at all times with respect to ζ and that at small times it is determined by a large number of derivatives; in the course of time, however, diffusion produces profiles which are determined adequately by only two axial derivatives. The species dependent distribution functions f_n are functions of η, χ, and τ only, and, from Equations (13) and (14), it can be seen that they obey the normalization condition

$$\langle f_n \rangle = \delta_{on} \tag{15}$$

Substituting Equation (13) into Equation (8), we have

$$\frac{\partial}{\partial \tau}\left(\sum_{n=0}^{\infty} f_n \frac{\partial^n \bar{c}_i}{\partial \zeta^n} \right) + (1 - \alpha_i - \chi^2 - \eta^2) \sum_{n=0}^{\infty} f_n \frac{\partial^{n+1} \bar{c}_i}{\partial \zeta^{n+1}}$$

$$+ \epsilon_i \sum_{n=0}^{\infty} \frac{\partial f_n}{\partial \eta} \cdot \frac{\partial^n \bar{c}_i}{\partial \zeta^n} = \sum_{n=0}^{\infty} \frac{\partial^2 f_n}{\partial \chi^2} \cdot \frac{\partial^n \bar{c}_i}{\partial \zeta^n} + \sum_{n=0}^{\infty} \frac{\partial^2 f_n}{\partial \eta^2}$$

$$\frac{\partial^n \bar{c}_i}{\partial \zeta^n} + \frac{1}{Pe_i^2} \sum_{n=0}^{\infty} f_n \cdot \frac{\partial^{n+2} \bar{c}_i}{\partial \zeta^{n+2}} \tag{16}$$

Averaging Equation (16) over the cross section, we get

$$\sum_{n=0}^{\infty} \frac{\partial^n \bar{c}_i}{\partial \zeta^n} \cdot \frac{\partial}{\partial \tau} \langle f_n \rangle + \sum_{n=0}^{\infty} \langle f_n \rangle \frac{\partial}{\partial \zeta}\left(\frac{\partial^n \bar{c}_i}{\partial \zeta^n} \right) + \sum_{n=0}^{\infty}$$

$$\langle (1 - \alpha_i - \chi^2 - \eta^2) f_n \rangle \frac{\partial^{n+1} \bar{c}_i}{\partial \zeta^{n+1}} + \sum_{n=0}^{\infty} \left\langle \epsilon_i \frac{\partial f_n}{\partial \eta} - \frac{\partial^2 f_n}{\partial \chi^2} \right.$$

$$\left. - \frac{\partial^2 f_n}{\partial \eta^2} \right\rangle \cdot \frac{\partial^n \bar{c}_i}{\partial \zeta^n} = \frac{1}{Pe_i^2} \sum_{n=0}^{\infty} \langle f_n \rangle \cdot \frac{\partial^{n+2} \bar{c}_i}{\partial \zeta^{n+2}} \tag{17}$$

The boundary condition (9) becomes, in terms of the distribution functions

$$\eta\left(\frac{\partial f_n}{\partial \eta} - \epsilon_i f_n \right) + \chi \frac{\partial f_n}{\partial \chi} = 0 \quad \text{at} \quad \eta^2 + \chi^2 = 1 \tag{18}$$

The second boundary condition is that the functions f_n are symmetric with respect to χ:

$$\frac{\partial f_n}{\partial \chi} = 0 \quad \text{at} \quad \chi = 0 \tag{19}$$

It follows from Equation (18) that

$$\left\langle \epsilon_i \frac{\partial f_n}{\partial \eta} - \frac{\partial^2 f_n}{\partial \chi^2} - \frac{\partial^2 f_n}{\partial \eta^2} \right\rangle = 0 \tag{20}$$

Integrating Equation (13) over z from $-\infty$ to $+\infty$, we get

$$f_0 = (\pi R^2) \frac{\int_{-\infty}^{+\infty} c_i dz}{\int_{-\infty}^{+\infty} \int_{-R}^{R} \int_{-\sqrt{R^2-y^2}}^{\sqrt{R^2-y^2}} c_i dx dy dz} \tag{21}$$

From Equations (11) and (21) it follows that

$$\alpha_i = \langle (1 - \chi^2 - \eta^2) f_0 \rangle \tag{22}$$

Substituting Equations (15), (18), and (20) into Equation (17), we obtain

$$\frac{\partial \bar{c}_i}{\partial \tau} = \frac{1}{Pe_i^2} \cdot \frac{\partial^2 \bar{c}_i}{\partial \zeta^2} - \sum_{n=1}^{\infty} \langle 1 - \alpha_i - \chi^2 - \eta^2) f_n \rangle \frac{\partial^{n+1} \bar{c}_i}{\partial \zeta^{n+1}} \tag{23}$$

DETERMINATION OF THE DISTRIBUTION FUNCTIONS

Substituting Equation (23) into Equation (16) and collecting the coefficients of the axial derivatives of c_i for each value of n, we have

$$\sum_{n=0}^{\infty} \left\{ \left[\frac{\partial f_n}{\partial \tau} - \sum_{m=0}^{n-2} f_m (1 - \alpha_i - \chi^2 - \eta^2) f_{n-m-1} \right.\right.$$

$$\left. + (1 - \alpha_i - \chi^2 - \eta^2) f_{n-1} \right.$$

$$\left.\left. + \left(\epsilon_i \frac{\partial f_n}{\partial \eta} - \frac{\partial^2 f_n}{\partial \chi^2} - \frac{\partial^2 f_n}{\partial \eta^2} \right) \right] \frac{\partial^n c_i}{\partial \zeta^n} \right\} = 0 \tag{24}$$

where

$$f_n \equiv 0 \quad \text{for} \quad n < 0 \tag{25}$$

Equation (24) is satisfied by

$$\frac{\partial f_n}{\partial \tau} + \epsilon_i \frac{\partial f_n}{\partial \eta} - \frac{\partial^2 f_n}{\partial \eta^2} - \frac{\partial^2 f_n}{\partial \chi^2} = \sum_{m=0}^{n-2}$$

$$[f_m \langle (1 - \alpha_i - \chi^2 - \eta^2) f_{n-m-1} \rangle]$$

$$- (1 - \alpha_i - \chi^2 - \eta^2) f_{n-1} \tag{26}$$

In particular

$$\frac{\partial f_0}{\partial \tau} + \epsilon_i \frac{\partial f_0}{\partial \eta} - \frac{\partial^2 f_0}{\partial \eta^2} - \frac{\partial^2 f_0}{\partial \chi^2} = 0 \tag{27}$$

and

$$\frac{\partial f_1}{\partial \tau} + \epsilon_i \frac{\partial f_1}{\partial \eta} - \frac{\partial^2 f_1}{\partial \eta^2} - \frac{\partial^2 f_1}{\partial \chi^2} = -(1 - \alpha_i - \chi^2 - \eta^2) f_0 \tag{28}$$

The initial condition on the distribution functions f_n is, from Equation (5)

$$f_n(\tau, \eta, \chi) = \delta_{on} \quad \text{at} \quad \tau = 0 \tag{29}$$

From Equations (26) to (28) it should be clear that the distribution functions $\{f_n\}$ are determined successively by solving for each f_n a Sturm-Liouville boundary value problem. The differential equation for each $f_n (n > 1)$ involves inhomogeneous terms comprising the lower elements of the hierarchy as seen from Equations (27) and (28). The Sturm-Liouville operator and the boundary conditions are identical for each f_n, and we will exploit this in what follows.

Let us define the operator

$$L \equiv \epsilon_i \frac{\partial}{\partial \eta} - \frac{\partial^2}{\partial \eta^2} - \frac{\partial^2}{\partial \chi^2} \tag{30}$$

on a domain $D(L)$ consisting of functions satisfying boundary conditions (18) and (19), and let

$$\{\lambda_j, \Lambda_j\} \quad j = 1, \ldots, \infty$$

be the set of eigenvalues and eigenvectors of L:

$$(L - \lambda_j)\Lambda_j = 0 \tag{31}$$

It can be readily shown that the operator L is symmetric in $D(L)$ with respect to the inner product:

$$(\Lambda_k; \Lambda_j) \equiv \int\int_{\chi^2+\eta^2 \leq 1} e^{-\epsilon_i \eta} \Lambda_k \Lambda_j d\chi d\eta \tag{32}$$

Λ_k and Λ_j are eigenfunctions of L, and L is positive semidefinite. It follows, then, that eigenfunctions corresponding to distinct eigenvalues are orthogonal with respect to the same inner product.

Equation (26) can be cast in the form

$$\frac{\partial f_n}{\partial \tau} + L f_n = g_n \tag{33}$$

where, in particular

$$g_0 = 0 \tag{34}$$

and

$$g_1 = -f_0(1 - \alpha_i - \chi^2 - \eta^2) \tag{35}$$

Expanding f_n in the set of eigenfunctions of L, we have

$$f_n = \sum_{j=0}^{\infty} C_{nj}(\tau) \Lambda_j(\eta, \chi) \tag{36}$$

Performing the inner product (32) with Λ_k and Equation (33), we get

$$\frac{\partial}{\partial\tau}(\Lambda_k; f_n) + \lambda_k(\Lambda_k; f_n) = (\Lambda_k; g_n) \tag{37}$$

from where

$$(\Lambda_k; f_n) = e^{-\lambda_k\tau}\left\{\int_0^\tau (\Lambda_k; g_n)e^{\lambda_k\tau}d\tau' + (\Lambda_k; f_n)|_{\tau=0}\right\} \tag{38}$$

Performing the same inner product with Equation (36), we get

$$C_{nk}(\tau) = (\Lambda_k; f_n) \tag{39}$$

If the eigenfunctions are normalized, that is if

$$\int\int_{\chi^2+\eta^2\leq 1} e^{-\epsilon_i\eta}\Lambda_k^2 d\chi d\eta = 1 \tag{40}$$

then, from Equation (36)

$$f_n = \sum_{n=0}^{\infty}\left\{\left[\int_0^\tau (\Lambda_j; g_n)e^{-\lambda_j(\tau-\tau')}d\tau' + (\Lambda_j; f_n)|_{\tau=0}e^{-\lambda_j\tau}\right]\Lambda_j\right\} \tag{41}$$

In particular, from Equations (29) and (34)

$$f_0 = \sum_{j=0}^{\infty}\left\{\int\int_{\chi^2+\eta^2\leq 1}[e^{-\epsilon_i\eta}\Lambda_j d\chi d\eta]e^{-\lambda_j\tau}\Lambda_j\right\} \tag{42}$$

It is clear from Equation (42) that the steady state part of f_0, $\overline{f_0}$ corresponds to the null eigenvalue which we will call λ_1. It can be immediately seen from Equation (31) that the corresponding eigenvector Λ_1 is

$$\Lambda_1 = \frac{e^{\epsilon_i\eta}}{N_1} \tag{43}$$

where N_1 is the normalization constant which, from Equation (40), is

$$N_1 = \left(\frac{2\pi I_1(\epsilon_i)}{\epsilon_i}\right)^{1/2} \tag{44}$$

From Equation (42) we have

$$\overline{f_0} = \left(\int\int_{\chi^2+\eta^2\leq 1} e^{-\epsilon_i\eta}\Lambda_1 d\chi d\eta\right)\Lambda_1 = \frac{\pi e^{\epsilon_i\eta}}{N_1^2} = \frac{\epsilon_i e^{\epsilon_i\eta}}{2I_1(\epsilon_i)} \tag{45}$$

From Equations (29), (41), and (43) we have

$$f_n = \sum_{n=2}^{\infty}\left\{\left[\int_0^\tau (\Lambda_j; g_n)e^{-\lambda_i(\tau-\tau')}d\tau\right]\Lambda_j\right\} + \frac{C_{n1}e^{\epsilon_i\eta}}{N_1} \tag{46}$$

The orthogonality of the eigenfunctions implies that

$$<\Lambda_j> = 0, \quad j > 1 \tag{47}$$

It follows, then, from Equations (15) and (46) that

$$C_{n1} = 0, \quad n > 1 \tag{48}$$

Equations (46) and (48) give, in particular

$$f_1 = -\sum_{j=2}^{\infty}\left\{\left[\int_0^\tau\left(\int\int_{\chi^2+\eta^2<1} e^{-\epsilon_i\eta}[\Lambda_j; (1-\alpha_i-\chi^2-\eta^2)f_0]d\chi d\eta\right)e^{-\lambda_j(\tau-\tau')}d\tau'\right]\Lambda_j\right\} \tag{49}$$

The inner product in Equation (49) may be written as

$$[\Lambda_j; (1-\alpha_i-\chi^2-\eta^2)f_0] = \sum_{m=2}^{\infty} F_{mj}e^{-\lambda_m\tau} + D_j \tag{50}$$

where

$$F_{mj} \equiv (\Lambda_m; 1)\cdot[\Lambda_j; (1-\alpha_i-\chi^2-\eta^2)\Lambda_m] \tag{51}$$

and

$$D_j = \frac{\pi}{N_1^2}\cdot[\Lambda_j; (1-\alpha_i-\chi^2-\eta^2)e^{\epsilon_i\eta}] \tag{52}$$

Substituting Equation (50) into Equation (49) and integrating over time, we get

$$f_1 = -\sum_{j=2}^{\infty}\left\{e^{-\lambda_j\tau}\sum_{\substack{m=2\\ m\neq j}}^{\infty}\frac{F_{mj}[e^{(\lambda_j-\lambda_m)\tau}-1]}{\lambda_j-\lambda_m} + F_{jj}\tau e^{-\lambda_j\tau} - \frac{D_j}{\lambda_j}(e^{-\lambda_j\tau}-1)\Lambda_j\right\} \tag{53}$$

It is clear from Equation (53) that the steady state part of f_1, $\overline{f_1}$ is

$$\overline{f_1} = -\sum_{j=2}^{\infty}\frac{D_j}{\lambda_j}\Lambda_j = \frac{\pi}{N_1^2}\cdot\sum_{j=2}^{\infty}\frac{[\Lambda_j; (\chi^2+\eta^2)e^{\epsilon_i\eta}]}{\lambda_j}\Lambda_j \tag{54}$$

The preceding, somewhat lengthy treatment may be condensed into the following alternative version, which provides a perspective view of the calculations of $\{f_n\}$.

We denote by operator G, the inverse of the transient operator $(\partial/\partial\tau + L)$, where L is the earlier Sturm-Liouville operator with domain $D(L)$. The operation of G on any function of χ and η, square integrable in the unit circle $\chi^2+\eta^2 = 1$ for every τ, may be represented by

$$Gf(\chi, \eta, \tau) \equiv \int_0^\tau d\tau' \int\int_{\chi^2+\eta^2\leq 1} d\chi' d\eta' G(\chi, \eta, \tau; \chi', \eta', \tau')[e^{-\epsilon_i\eta'}f(\chi', \eta', \tau')] \tag{55}$$

The transformed function has zero initial value as is required for the solution of Equation (33) written for $n \geq 1$. The kernel $G(\chi, \eta, \tau; \chi', \eta', \tau')$ is given by

$$G(\chi, \eta, \tau; \chi', \eta', \tau') = \sum_{k=0}^{\infty} e^{-\lambda_k(\tau-\tau')}\Lambda_k(\chi, \eta)\Lambda_k(\chi', \eta') \tag{56}$$

where (λ_k, Λ_k) are the set of eigenvalues and normalized eigenvectors of L. The solution of Equation (33) is given by

$$f_n = Gg_n \quad n \geq 1 \tag{57}$$

The function f_0 has nonzero initial value and has been obtained by solving the homogeneous Equation (33) since $g_0 = 0$. Clearly, successive applications of the operator G will produce as many f_n's as needed. We have, however, terminated our computations at f_1. The eigenvalues and eigenvectors of L are not calculable analytically, since the operator is not separable so that variational estimates have been used. These are considered in the next section.

COMPUTATION OF THE EIGENVALUES AND EIGENFUNCTIONS OF THE OPERATOR L

The eigenvalue problem is defined by Equation (31). The lowest eigenvalue and the corresponding eigenfunction can easily be determined analytically:

$$\lambda_1 = 0 \tag{58}$$

$$\Lambda_1 = \frac{e^{\epsilon_i \eta}}{N_1} \tag{59}$$

The other eigenvalues and eigenfunctions can be determined analytically only in the limit where ϵ_i is zero. For the general case of nonzero ϵ_i, we will seek numerical approximations of the remaining eigenvalues and eigenfunctions.

For the particular case where

$$\epsilon_i = 0 \tag{60}$$

the eigenfunctions can be readily computed as

$$\Lambda_j{}^0 = \frac{J_0(a_j r)}{N_j{}^0}, \quad j = 1, \ldots, \infty \tag{61}$$

and the eigenvalues are

$$\lambda_j{}^0 = a_j{}^2, \quad j = 1, \ldots, \infty \tag{62}$$

In the case where $\epsilon_i \neq 0$, the Rayleigh-Ritz method (Weinberger, 1972) will be used to obtain estimates $\lambda_j{}^*$ for the eigenvalues and approximations for the eigenfunctions. The Rayleigh-Ritz method approximates the eigenfunction Λ_j with the linear combination

$$\mathbf{\Lambda}_j{}^* = \sum_{k=1}^{N} \alpha_{jk} \omega_k \tag{63}$$

where ω_k, with $k = 1, \ldots, N$, is a set of N linearly independent functions which satisfy the boundary conditions of the eigenvalue problem being solved, and α_{jk}, with $j = 1, \ldots, N$ and $k = 1, \ldots, N$, is a set of constants. The choice of the functions ω_k is usually very important for the success of the approximation, a good choice resulting in a good approximation with a small number of functions ω_k and a bad choice requiring a large number of such functions for a satisfactory result.

We chose the functions

$$\omega_k = \frac{1}{M_k} e^{\epsilon_i \eta} J_0(a_k r) \tag{64}$$

to approximate the eigenfunctions by the Rayleigh-Ritz method. The functions defined by Equation (64) are symmetric functions with respect to χ which satisfy the boundary condition (18). Besides the fundamental requirement of satisfying the boundary conditions, the chosen functions have some attractive features:

1. The first function ω_1 is an eigenfunction of the problem, and it follows then that

$$\alpha_{1k} = \delta_{1k}$$

2. In the limit where $\epsilon_i = 0$, the functions ω_k become the eigenfunctions of the problem.

To apply the Rayleigh-Ritz method, we define the $N \times N$ matrices $\mathbf{A}$ and $\mathbf{B}$:

$$A_{ij} \equiv (\omega_i; L\omega_j) = \frac{a_i a_j}{M_i M_j} \int_0^1 L(\epsilon_i r) J_1(a_i r) J_1(a_j r) r dr \tag{65}$$

and

$$B_{ij} \equiv (\omega_i; \omega_j) = \frac{1}{M_i M_j} \int_0^1 L(\epsilon_i r) J_0(a_i r) J_0(a_j r) r dr \tag{66}$$

where

$$L(x) = \int_0^{2\pi} e^{x\cos\theta} d\theta = 2\pi I_0(x) \tag{67}$$

The integrals (65) and (66) were computed numerically.

The N dimensional eigenvalue problem

$$(\mathbf{A} - \lambda_j{}^* \mathbf{B}) \mathbf{\Lambda}_j{}^* = 0 \tag{68}$$

is then formulated. The eigenvalues $\lambda_j{}^*$ of the problem (68) are the Rayleigh-Ritz upper bounds of the eigenvalues of the operator L. The components of the eigenvectors $\mathbf{\Lambda}_j{}^*$ are the coefficients α_{jk} appearing in Equation (63).

The eigenvalues of problem (68) are those of matrix $\mathbf{A} \cdot \mathbf{B}^{-1}$; the eigenvectors of problem (68) are those of $\mathbf{A} \cdot \mathbf{B}^{-1}$ premultiplied by $\mathbf{B}^{-1}$.

NUMERICAL RESULTS

Numerical results were obtained with the help of a truncated form of Equation (23), usually referred to as the dispersion model:

$$\frac{\partial \bar{c}_i}{\partial \tau} = \left[\frac{1}{Pe_i{}^2} + \langle (\chi^2 + \eta^2) f_1 \rangle \right] \frac{\partial^2 \bar{c}_i}{\partial \zeta^2} \tag{69}$$

In order to solve Equation (69), we need α_i, used in the definition of ζ, and the dimensionless dispersion coefficient

$$\frac{\mathcal{D}_{i,eff}}{\mathcal{D}_{im} Pe_i{}^2} \equiv \mathbb{D}_i = \frac{1}{Pe_i{}^2} + \langle (\chi^2 + \eta^2) f_1 \rangle \tag{70}$$

From Equations (15), (22), and (45) we get for the steady state part of α_i, $\bar{\alpha}_i$

$$\bar{\alpha}_i = 1 - \langle (\chi^2 + \eta^2) \bar{f}_0 \rangle = \frac{2}{\epsilon_i} \cdot \frac{I_2(\epsilon_i)}{I_1(\epsilon_i)} \tag{71}$$

The retardation coefficient defined by Equation (2) is then at the steady state

$$r_i = \frac{\epsilon_i}{4} \cdot \frac{I_1(\epsilon_i)}{I_2(\epsilon_i)} \tag{72}$$

For planar-channel EPC, we have (Reis, 1976*a*)

$$r_i = \frac{\epsilon_i}{3\left(\coth \epsilon_i - \frac{1}{\epsilon_i}\right)} \tag{73}$$

In Figure 2, $v_0/\langle v_i \rangle$ is plotted against ϵ_i as a full line for hollow fiber EPC (where $v_0/\langle v_i \rangle = 2r_i$) and as a dashed line for planar-channel EPC (where $v_0/\langle v_i \rangle = 3r_i/2$) to stress the similarity of performance of the

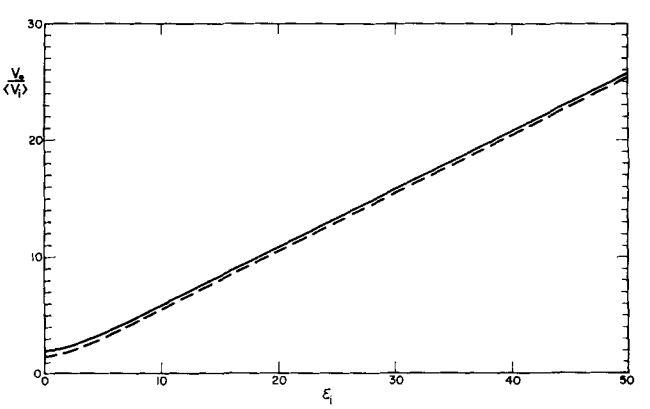

Fig. 2. Retardation as a function of the polarization Péclet number. The solid line refers to hollow fiber EPC, and the dashed one to its planar counterpart. In both cases, v_0 is the maximum solvent velocity.

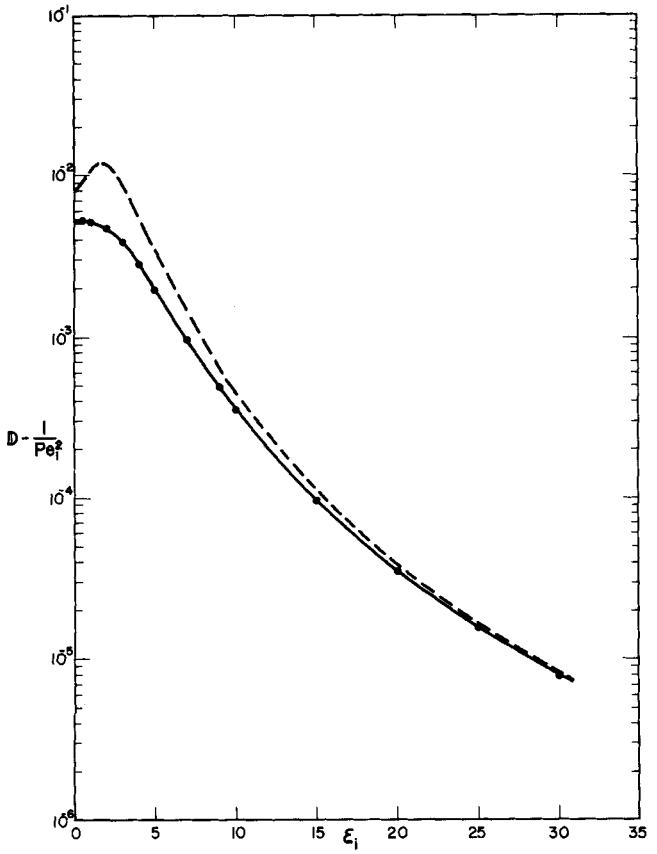

Fig. 3. Dimensionless dispersion coefficient as a function of the polarization Péclet number. The solid and dashed lines refer to hollow fiber and planar EPC, respectively. Dots refer to points calculated.

two processes when mean species velocity is scaled relative to maximum solvent velocity.

From Equations (14), (32), and (54), it follows that

$$\mathbb{D}_i - \frac{1}{Pe_i^2} = <(\chi^2 + \eta^2)\bar{f}_1> = \left(\frac{\pi}{N_1}\right)^2 \sum_{j=2}^{\infty} \frac{<(\chi^2 + \eta^2)\Lambda_j>^2}{\lambda_j} \tag{74}$$

Using the Rayleigh-Ritz estimates of Λ_j and λ_j, we get

$$<(\chi^2 + \eta^2)\bar{f}_1> \doteq \left(\frac{\pi}{N_1}\right)^2 \sum_{j=2}^{N} \frac{\left(\sum_{m=1}^{N} \alpha_{jm} V_m\right)^2}{N_j^* \lambda_j^*} \tag{75}$$

where

$$V_m = \frac{\int_0^1 I_0(\epsilon_i r) J_0(a_m r) r^3 dr}{\pi \left(\int_0^1 I_0(\epsilon_i r) J_0^2(a_m r) r dr\right)^{1/2}} \tag{76}$$

and

$$N_j^* = \left\{ \sum_{n,l=1}^{N} \alpha_{jn}\alpha_{jl} \frac{\int_0^1 I_0(\epsilon_i r) J_0(a_n r) J_0(a_l r) r dr}{\left[\int_0^1 I_0(\epsilon_i r) J_0^2(a_n r) r dr \int_0^1 I_0(\epsilon_i r) J_0^2(a_l r) r dr\right]^{1/2}} \right\} \tag{77}$$

In the limit where $\epsilon_i = 0$, we have

$$\mathbb{D}_i - \frac{1}{Pe_i^2} = 16 \sum_{j=2}^{\infty} \frac{1}{a_j^6} = \frac{1}{192} \tag{78}$$

For planar-channel EPC, we have (Reis, 1976*a*)

$$\mathbb{D}_i - \frac{1}{Pe_i^2} = \frac{8}{\epsilon_i^2}\left[\frac{1}{3}(\coth^2 \epsilon_i - 1) + \frac{1}{\epsilon_i}(\coth \epsilon_i - \coth^3 \epsilon_i) + \frac{1}{\epsilon_i^2}(2 - \coth^2 \epsilon_i) - \frac{5}{\epsilon_i^3}\coth \epsilon_i + \frac{7}{\epsilon_i^4}\right] \tag{79}$$

which, for $\epsilon_i > 10$, is well approximated by

$$\mathbb{D} - \frac{1}{Pe_i^2} \doteq \frac{8}{\epsilon_i^4}\left(1 - \frac{5}{\epsilon_i} + \frac{7}{\epsilon_i^2}\right) \tag{80}$$

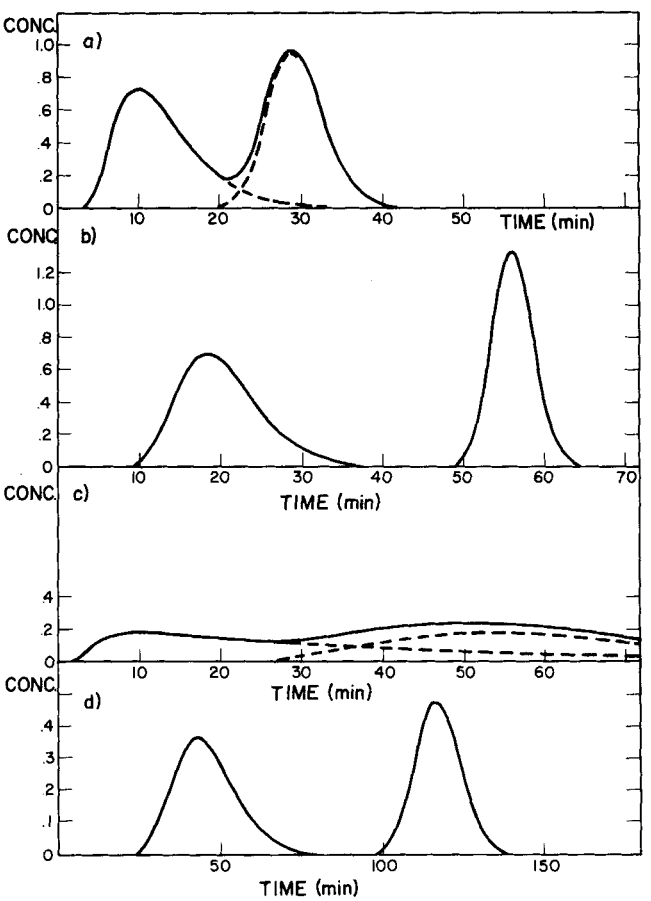

Fig. 4. Separation of polyelectrolytes injected as a mixed pulse. Solute A corresponds closely to human serum albumin with mobility and diffusivity of 5.9 × 10^{-5} cm²/V-s and 6.1 × 10^{-7} cm²/s, respectively; B corresponds to human gamma globulin with values of 1.2 × 10^{-5} and 4.0 × 10^{-7}. Figure 4*a* represents prediction for $E = 5$ V/cm, $R = 0.04$ cm, and $L/v_0 = 167$ s; Figure 4*b* is for similar conditions except $E = 10$ V/cm. Figure 4*c* is for the conditions of (a) except $R = 0.08$ cm; Figure 4*d* is for the conditions of (a) except $L/v_0 = 668$ s.

In Figure 3, $\mathbb{D} - 1/Pe_i^2$ is plotted as a function of ϵ_i for both hollow fiber EPC (full line) and planar-channel EPC (dashed line). The first seven eigenvalues provide sufficient accuracy for values of ϵ_i up to 10. For values of ϵ_i between 10 and 50, fifteen eigenvalues were computed.

Figures 2 and 3 show that hollow fiber EPC and planar-channel EPC have the same asymptotic behavior if the maximum convection velocity is used as a scaling factor for $<v_i>$.

Figure 4 shows the response of hollow fiber EPC to a pulse injection of a binary mixture, as predicted by the model described above. Once steady state is reached, the resolution of two species depends on three operation variables: electric field, hollow fiber radius, and the ratio L/v_0. Figure 4 shows the effect of those operation variables. The components of the binary mixture chosen for the simulation represented in Figure 4 have the electrophoretic mobility and diffusivity of human serum albumin and human gamma globulin in barbital at pH 8.6.

DISCUSSION

The primary motivation for this study was to characterize hollow fiber electropolarization chromatography (EPC) as a research tool and in particular to determine the effect of boundary curvature on convective dispersion. The results were sufficient for this purpose and are also found to be useful for other reasons which did not come to mind until later. These include both the description of other possibly interesting physical situations and intrinsic value of the mathematical techniques developed.

The potential attractiveness of hollow fiber EPC was demonstrated by Reis and Lightfoot in 1976 and is illustrated here in Figure 4. At that time we were not, however, able to determine how much of the observed dispersion was intrinsic to the process and how much resulted from mixing processes in the auxiliary equipment. The above analysis is doubly useful in this respect in providing a means of calculating effective dispersion and in showing that for most purposes of expected interest, a simple boundary-layer approximation is satisfactory for this purpose. Thus, Equation (79) may be used for ϵ_i greater than about 10, and under these conditions it may be approximated by Equation (80) which has already been given by Lee and Lightfoot (1976) for ultrafiltration induced polarization chromatography. It may be seen from this limiting result, or from Figure 2, that very low dispersion and hence very sharp separations are possible at high polarization Péclet numbers.

In a forthcoming paper we shall show that all separations obtained to date are dominated by dispersion in the auxiliary apparatus and that much of this auxiliary dispersion can be eliminated by proper design of the separation system.

The above analysis also describes a number of other physical situations of possible chemical engineering interest. These include polarization chromatography using other cross flows or fields and the gravitational settling of dilute suspensions in Poiseuille flow. Such settling occurs in a number of important situations but usually at high particle concentrations or in turbulent flow. It is by no means certain that the technique introduced in this paper can be extended to such situations, but this appears to be a possibility worth investigating.

More generally, it appears that the use made of functional analysis in this development can be extended to a variety of other geometries and to quite different specific problems.

ACKNOWLEDGMENT

The authors are indebted for financial support to the National Science Foundation Grant ENG 75-05456. In addition, J. F. G. Reis wishes to acknowledge assistance provided by Fundaçao Calouste Gulbenkian.

NOTATION

a_i = zeros of J_1, the Bessel function of order 1
$\underline{\mathbf{A}}$ = matrix with elements defined as by Equation (65)
$\underline{\mathbf{B}}$ = matrix with elements defined as by Equation (66)
c_i = molar concentration of species i
C_i = constant
$\bar{c}_i$ = cross-sectional average concentration of species i
C_{nj} = coefficients of the expansion of f_n in eigenfunctions Λ_j
D_j = expressions as defined by Equation (52)
$\mathcal{D}_{im}$ = pseudo binary diffusion coefficient of species i
$\mathbb{D}_i$ = dimensionless dispersion coefficient, as defined by Equation (70)
$\mathcal{D}_{i,eff}$ = dispersion coefficient $= \mathcal{D}_{im} Pe_i^2 \mathbb{D}_i$
$\mathbf{E}$ = electrical field
E_x, E_y = components of $\mathbf{E}$
F_{mj} = expressions as defined by Equation (51)
f_n = species dependent distribution functions (of η, χ, and τ)
$\bar{f}_n$ = steady state part of f_n
g_n = inhomogeneous term, as defined by Equation (33)
G = inverse of the operator $(\partial/\partial\tau + L)$
I_n = hyperbolic Bessel function of order n
J_i = Bessel function of order i
L = differential operator as defined by Equation (30)
m_i = electrophoretic mobility of species i
M_i = normalization constants for approximation function ω_i
N = number of approximation functions used in the Rayleigh-Ritz technique
N_i = normalization constant of eigenfunction Λ_i
N_i^* = normalization constant of eigenvector Λ_i^*
$Pe_i \equiv v_0 R/\mathcal{D}_{im}$ = convection Péclet number
R = inner radius of the hollow fiber
r = radial coordinate
r_i = retardation coefficient, as defined by Equation (2)
S = hollow fiber cross section
t = time
v = axial component of the molar average velocity
$<v_i>$ = cross-sectinnal average axial velocity of species i
$<x>$ = cross-sectional average of the molar average velocity
v_0 = maximum axial velocity
x = rectangular coordinate
y = direction of the electrical field
z = axial direction

Greek Letters

α_i = dimensionless velocity of the center of mass of species i, as defined by Equation (11)
$\bar{\alpha}_i$ = steady state value of α_i
α_{jk} = expansion coefficients, as defined by Equation (63)
$\delta(z)$ = Dirac delta
δ_{ij} = Kronecker delta
$\epsilon_i \equiv m_i E_y R/\mathcal{D}_{im}$ = polarization Péclet number (in planar EPC, R is the half width of the channel).
ζ = dimensionless axial coordinate, as defined by Equation (12)

η = y/R
λ_i = eigenvalues of L
λ_i^0 = eigenvalues of L when $\epsilon_i = 0$
λ_i^* = Rayleigh-Ritz estimate of λ_i
Λ_i = eigenfunctions of L
Λ_i^0 = eigenfunctions of L when $\epsilon_i = 0$
Λ_i^* = Rayleigh-Ritz estimate of Λ_i
τ = $t\,\mathcal{D}_{im}/R^2$
χ = x/R
ω_i = approximation functions as defined by Equation (64)

LITERATURE CITED

Gill, W. N., and R. Sankarasubramanian, "Exact Analysis of Unsteady Convection Diffusion," *Proc. Royal Soc.*, **A316**, 341 (1970).

Lee, H.-L., and E. N. Lightfoot, "Preliminary Report on Ultrafiltration-Induced Polarization Chromatography—An Analog of Field-Flow Fractionation," *Sep. Sci.*, **11**, No. 5, 417 (1976).

Reis, J. F. G., and E. N. Lightfoot, "Electropolarization Chromatography," *AIChE J.*, **22**, No. 4, 779 (1976).

Reis, J. F. G., "Separation Processes Based on Electromigration for Fractionation of Proteins," Ph.D. dissertation, Univ. Wisc., Madison (1976*a*).

Weinberger, H. F., "Variational Methods for Eigenvalue Approximation," Society for Industrial and Applied Mathematics, Philadelphia (1972).

Manuscript received June 30, 1977; revision received January 23, and accepted February 22, 1978.

Phase-Plane Analysis of Feedback Control of Unstable Steady States in a Biological Reactor

DAVID DIBIASIO
HENRY C. LIM
WILLIAM A. WEIGAND
and
GEORGE T. TSAO

School of Chemical Engineering
Purdue University
West Lafayette, Indiana 47907

Feedback control of an open loop, unstable, continuous flow, stirred-tank biological reactor was investigated theoretically using several microbial growth models. The closed loop system can be made globally stable, but constraints on the manipulated variable can lead to as many as five steady states, which are either saddle points or locally stable nodes.

SCOPE

Under certain conditions, multiple steady states are possible for continuous cultivation of a pure culture (Yano and Koga, 1969). In such cases, one of the steady states is unstable. When modeling the growth kinetics of microorganisms or designing microbial reactors, it is necessary to specify the specific growth rate of the organism as a function of substrate concentration over the range of possible concentrations. To obtain this data from continuous culture, one must attain operation at unstable steady states. In practical applications (that is, production of single-cell protein, SCP), it may be desirable to operate at or near the maximum specific growth rate for optimal cell production. Such an operation would require knowledge of the system behavior at unstable steady states. It might also be conceivable that an SCP process, with a series of reactors, could be optimized by operating one or more reactors at an unstable steady state. The most expedient means of operation at an unstable steady state is through the application of conventional feedback control. Thus, the study of unstable steady states in the CSTBR plays an important role in the research and design of microbial reactors.

The objective of this paper is to present the results of a theoretical study of the control of unstable steady states in a CSTBR. A number of kinetic models are used in examining the existence of multiple states in the open loop process and the operation at unstable steady states in the closed loop system. The possibility of multiple steady states in the closed loop system will be examined.

The models examined are a classical substrate inhibition model (Yano and Koga, 1969; Edwards et al., 1972), a variable yield model (Chen et al., 1976), a first-order lag model adopted from Young et al. (1970), and a wall growth model (Howell et al., 1972).

Edwards et al. (1972) presented a theoretical study of the control of stable steady states in a CSTBR. Phase-plane analysis was used to show that feedback control could eliminate the instabilities in the system. In a more recent experimental study, Ko and Edwards (1975) demonstrated

Correspondence concerning this paper should be addressed to Henry C. Lim.